Synthesis and Applications of Cyano-Vinylene-Based Polymers Containing Cyclopentadithiophene and Dithienosilole Units for Photovoltaic Cells

HARIHARA PADHY,[1] DURYODHAN SAHU,[2] DHANANJAYA PATRA,[1] MURALI KRISHNA POLA,[1] JEN-HSIEN HUANG,[2] CHIH-WEI CHU,[2,3] KUNG-HWA WEI,[1] HONG-CHEU LIN[1]

[1]Department of Materials Science and Engineering, National Chiao Tung University, Hsinchu, Taiwan, Republic of China

[2]Research Center for Applied Sciences, Academia Sinica, Taipei, Taiwan, Republic of China

[3]Department of Photonics, National Chiao Tung University, Hsinchu, Taiwan, Republic of China

Received 1 April 2011; accepted 14 May 2011
DOI: 10.1002/pola.24779
Published online 31 May 2011 in Wiley Online Library (wileyonlinelibrary.com).

ABSTRACT: Two β-cyano-thiophenevinylene-based polymers containing cyclopentadithiophene (**CPDT-CN**) and dithienosilole (**DTS-CN**) units were synthesized via Stille coupling reaction with $Pd(PPh_3)_4$ as a catalyst. The effects of the bridged atoms (C and Si) and cyano-vinylene groups on their thermal, optical, electrochemical, charge transporting, and photovoltaic properties were investigated. Both polymers possessed the highest occupied molecular orbital (HOMO) levels of about −5.30 eV and the lowest unoccupied molecular orbital (LUMO) levels of about −3.60 eV, and covered broad absorption ranges with narrow optical band gaps (ca. 1.6 eV). The bulk heterojunction polymer solar cell (PSC) devices containing an active layer of electron-donor polymers (**CPDT-CN** and **DTS-CN**) blended with an electron-acceptor, that is, [6,6]-phenyl-C_{61}-butyric acid methyl ester ($PC_{61}BM$) or [6,6]-phenyl-C_{71}-butyric acid methyl ester ($PC_{71}BM$), in different weight ratios were explored under 100 mW/cm^2 of AM 1.5 white-light illumination. The PSC device based on **DTS-CN**:$PC_{71}BM$ (1:2 w/w) exhibited a best power conversion efficiency (PCE) value of 2.25% with V_{oc} = 0.74 V, J_{sc} = 8.39 mA/cm^2, and FF = 0.36. © 2011 Wiley Periodicals, Inc. J Polym Sci Part A: Polym Chem 49: 3417–3425, 2011

KEYWORDS: conjugated polymers; copolymerization; donor-acceptor; heteroatom-containing polymers; solar cells

INTRODUCTION Till now, polymer solar cells (PSC), composed of bicontinuous intermixing of electron donors and acceptors, have played a leading role in obtaining higher efficiencies as these devices allow the photogenerated electron-hole pairs to be efficiently separated throughout the bulk films and transported to the electrodes.[1] Though the conventional blends of poly(3-hexylthiophene) (P3HT) and [6,6]-phenyl-C_{61}-butyric acid methyl ester ($PC_{61}BM$) have reached power conversion efficiency (PCE) up to 5%,[2] further increase is rather difficult due to their limited photocurrent generation and intrinsic absorption properties. Therefore, an alternative approach to have better performance is to use low band gap (LBG) donor–acceptor (D–A) polymeric materials, and higher efficiencies up to 7.7% were obtained by such polymers.[3]

Recently, it remains a key challenge to design and synthesize new ideal LBG polymers with high intrinsic conductivities to develop their potential applications in highly efficient bulk-heterojunction (BHJ) solar cells by blending with an electron-acceptor like PCBM.[4–6] To increase the PCE in BHJ solar cells, some important characteristics of LBG polymers need to be dealt, such as: (i) a more favorable overlap of the absorption spectrum of the active layer with the solar emission for better solar photon harvesting,[7] (ii) a better charge carrier mobility,[8] and (iii) an optimized relative positions of the energy levels of the electron donors and acceptors[9] for the maximization of the open circuit voltage (V_{oc}) and better charge separation between electron–donor polymers and electron–acceptor PCBM. Furthermore, an ideal donor polymer should exhibit a band gap between 1.2 and 1.9 eV, which corresponds to a highest occupied molecular orbital (HOMO) energy level between −5.8 and −5.2 eV and a lowest unoccupied molecular orbital (LUMO) energy level between −4.0 and −3.8 eV.[10] To achieve higher efficiencies of BHJ solar cell devices, the difference of the LUMO levels between electron–donor polymer and electron–acceptor PCBM needs to be at least 0.3 eV.[11] Otherwise, the driving force for charge separation will be decreased, and also V_{oc} will be reduced by raising the HOMO level of the donor polymer. Therefore, in order to synthesize LBG polymers, the design rules described above suggest that the optimization of HOMO and LUMO levels of LBG polymers is the most promising strategy to develop BHJ solar cells with high efficiencies. However, it is difficult to synthesize the LBG

Correspondence to: H.-C. Lin (E-mail: linhc@mail.nctu.edu.tw)

polymers with all three properties like broad absorption spectra, high carrier mobilities, and appropriate molecular energy levels.

According to this D–A design, LBG polymers containing electron donating moieties from the 2,2′-bithiophene unit covalently bridged with an atom, such as C, N, S, and Si at 3,3′-position, have attracted considerable research attentions in recent days. The bridging atoms at 3,3′-position of donor moieties play an important role for LBG polymers in terms of solubility, planarity, band gap, and interchain packing, as well as for the performance of the BHJ solar cells.[12] Among these four donor units (i.e., 3,3′-C-, N-, S-, or Si-substituted 2,2′-bithiophene units), both dithienopyrrole and dithienothiophene had lower efficiencies in BHJ solar cells due to the low V_{oc} values arising from their high HOMO levels.[13] Thus, the LBG polymers containing the other two electron donating moieties, that is, cyclopentadithiophene and dithienosilole units, have emerged as potential materials for photovoltaic cells[14] due to their similar range of HOMO and LUMO levels as ideal polymers. In addition, to obtain the broad absorption band with high absorptivities of the conjugated polymers, electron-donating groups and/or electron-withdrawing groups are substituted on the main-chains of the conjugated polymers to raise the HOMO levels and/or to reduce the LUMO levels of the polymers.[15] Hence, introduction of electron-withdrawing cyano-vinylene groups to polymer backbones has several advantages, such as to lower the LUMO levels,[16] and tune their electro-optical properties,[17] and possess higher hole mobilities.[18] Recently, some polymers containing cyano-vinylene groups were applied to BHJ solar cells as photovoltaic materials.[19] However, the PCE values of these photovoltaic cells are still low at present. All these research results inspire us to incorporate cyano-vinylene electron-acceptors into the main-chains of conjugated polymers containing electron-donating cyclopentadithiophene and dithienosilole units for better photophysical, electrochemical, and photovoltaic properties. On the basis of this concept, soluble β-cyano-thiophenevinylene-based LBG D-A polymers (**CPDT-CN**, **DTS-CN**) containing cyclopentadithiophene- and dithienosilole units are designed and synthesized. The effects of the bridged atoms (i.e., C and Si) on the optical, electrochemical, charge transporting, and photovoltaic properties of the polymers are compared and reported in this study. A maximum PCE value of 2.25% could be reached by a PSC device containing an active layer of **DTS-CN**:$PC_{71}BM$. The preliminary study reveals that these LBG polymers may have potential applications in flexible electronic devices in the future.

EXPERIMENTAL

Materials

4,4-Bis(2-ethylhexyl)-cyclopenta[2,1-*b*:3,4-*b*′]dithiophene (**1**),[5(b)] 5-bromo-2-thiopheneacetonitrile (**3**),[18] 3,3′-di-*n*-hexylsilylene-2,2′-bithiophene (**4**),[14(e)] 4,4-Bis(2-ethylhexyl)-2,6-bis(trimethylstannanyl)-4H-cyclopenta-[2,1-b:3,4-b′]dithiophene (**6**),[5(b)] 5,5′-bis(trimethylstannyl)-3,3′-di-*n*-hexylsilylene-2,2′-bithiophene (**7**)[14(f)] were prepared according to the published methods. All other chemicals were purchased from Aldrich, ACROS, Fluka, or TCI. Toluene, tetrahydrofuran (THF), and diethyl ether were distilled over sodium/benzophenone. Chloroform ($CHCl_3$) was purified by refluxing with calcium hydride and then distilled. If not otherwise specified, the other solvents were degassed by nitrogen 1 h before use.

Measurements and Characterization

^1H and ^{13}C NMR spectra were measured using Varian Unity 300 MHz spectrometer. Elemental analyses were performed on a HERAEUS CHN-OS RAPID elemental analyzer. Thermogravimetric analyses (TGA) were conducted with a TA Instruments Q500 at a heating rate of 10 °C/min under nitrogen. The molecular weights of polymers were measured by gel permeation chromatography (GPC) using Waters 1515 separation module (concentration: 1 mg/1 mL in THF; flow rate: 1 mL/1 min), and polystyrene was used as a standard with THF as an eluant. UV-visible absorptions were recorded in dilute chloroform solutions (10^{-6} M) on a HP G1103A. Solid films of UV-vis measurements were spin-coated on a glass substrate from chlorobenzene solutions with a concentration of 10 mg/mL. Cyclic voltammetry (CV) measurements were performed using a BAS 100 electrochemical analyzer with a standard three-electrode electrochemical cell in a 0.1 M tetrabutylammonium hexafluorophosphate [(TBA)PF_6] solution (in acetonitrile) at room temperature with a scanning rate of 100 mV/s. During the CV measurements, the solutions were purged with nitrogen for 30 s. In each case, a carbon working electrode coated with a thin layer of polymers, a platinum wire as the counter electrode, and a silver wire as the quasi-reference electrode were used, and Ag/AgCl (3 M KCl) electrode was served as a reference electrode for all potentials quoted herein. The redox couple of ferrocene/ferrocenium ion (Fc/Fc^+) was used as an external standard. The corresponding highest occupied molecular orbital (HOMO) and lowest unoccupied molecular orbital (LUMO) levels were calculated using $E_{ox/onset}$ and $E_{red/onset}$ for experiments in solid films of polymers, which were performed by drop-casting films with the similar thickness from THF solutions (ca. 5 mg/mL). The onset potentials were determined from the intersections of two tangents drawn at the rising currents and background currents of the cyclic voltammetry (CV) measurements.

Fabrication of Polymer Solar Cells

The polymer solar cells in this study were composed of an active layer of blended polymers (**CPDT-CN** or **DTS-CN**:PCBM) in solid films, which was sandwiched between a transparent indium tin oxide (ITO) anode and a metal cathode. Before device fabrication, ITO-coated glass substrates (1.5×1.5 cm^2) were ultrasonically cleaned in detergent, deionized water, acetone, and isopropyl alcohol. After routine solvent cleaning, the substrates were treated with UV ozone for 15 min. Then, a modified ITO surface was obtained by spin-coating a layer of poly(ethylene dioxythiophene): polystyrenesulfonate (PEDOT:PSS; ~30 nm). After baking at 130 °C for 1 h, the substrates were transferred to a nitrogen-filled glove-box. Then, on the top of PEDOT:PSS layer, the active layer was prepared by spin coating from blended solutions of polymers **CPDT-CN** or **DTS-CN**:$PC_{61}BM$ (with 1:1 w/

w) and **DTS-CN**:$PC_{71}BM$ (with 1:1, 1:2, 1:3, w/w) subsequently with a spin rate of about 1000 rpm for 60 s, and the thickness of the active layer was typically about 80 nm. Initially, the blended solutions were prepared by dissolving both polymers and PCBM in 1,2-dichlorobenzene (20 mg/1 mL), followed by continuous stirring for 12 h at 50 °C. In the slow-growth approach, blended polymers in solid films were kept in the liquid phase after spin-coating by using the solvent with a high boiling point. Finally, a calcium layer (30 nm) and a subsequent aluminum layer (100 nm) were thermally evaporated through a shadow mask at a pressure below 6×10^{-6} Torr. The active area of the device was 0.12 cm^2. All PSC devices were prepared and measured under ambient conditions. The solar cell measurements were done inside a glove box under simulated AM 1.5G irradiation (100 mW/cm^2) using a Xenon lamp based solar simulator (Thermal Oriel 1000 W). The light intensity was calibrated by a mono-silicon photodiode with KG-5 color filter (Hamamatsu, Japan). The external quantum efficiency (EQE) spectra were obtained at short-circuit conditions. The light source was a 450 W Xe lamp (Oriel Instrument, model 6266) equipped with a water-based IR filter (Oriel Instrument, model 6123NS, Irvine, USA). The light output from the monochromator (Oriel Instrument, model 74100, Irvine, USA) was focused on the photovoltaic cell under test.

Fabrication of Hole- and Electron-Only Devices

The hole- and electron-only devices in this study contained, polymers **CPDT-CN** or **DTS-CN**:$PC_{61}BM$ (1:1 w/w) blend films sandwiched between transparent ITO anode and cathode. The devices have been prepared following the same procedure as the fabrication of BHJ devices, except that in the hole-only devices, Ca was replaced with MoO_3 ($\Phi = 5.3$ eV) and for the electron-only devices, the PEDOT:PSS layer was replaced with Cs_2CO_3 ($\Phi = 2.9$ eV). In hole-only devices, MoO_3 was thermally evaporated with a thickness of 20 nm and then capped with 50 nm of Al on the top of the active layer. On the other hand, Cs_2CO_3 was thermally evaporated in the electron-only devices with a thickness of ~2 nm on the top of transparent ITO. For both devices, annealing of the active layer was performed at 130 °C for 20 min. The space charge limited current (SCLC) method was used to evaluate the hole and electron mobilities of polymer blend films **CPDT-CN** or **DTS-CN**:$PC_{61}BM$ (1:1 w/w) by fabricating the hole- and electron-only devices. The electron and hole mobilities were determined precisely by fitting the plots of the dark current versus voltage (*J–V*) curves for single carrier devices to the SCLC model. The dark current is given by $J = 9\varepsilon_0\varepsilon_r\mu V^2/8L^3$, where $\varepsilon_0\varepsilon_r$ is the permittivity of the polymer, μ is the carrier mobility, and L is the device thickness.

Synthesis of Monomers and Polymers

4,4-Bis(2-ethylhexyl)-4H-cyclopenta[2,1-b:3,4-b] dithiophene-2,6-dicarbaldehyde (2)

A three-neck round-bottom flask containing 3.8 mL (50 mmol) of anhydrous DMF was cooled in an ice bath. To the solution, 4.7 mL (50 mmol) of phosphoryl chloride was added dropwise over a period of 20 min. 4,4-Bis(2-ethylhexyl)-cyclopenta[2,1-*b*:3,4-*b*′]dithiophene (**1**) (4.03 g, 10 mmol) in 30 mL of 1,2-dichloroethane was added to the above solution dropwise and heated to about 90 °C for 2 days. The solution was cooled to room temperature and then poured into ice cold saturated aqueous solution of sodium acetate (200 mL). Then, the mixture was extracted with CH_2Cl_2/water. The organic layer was concentrated under reduced pressure. Finally, the crude product was purified by column chromatography using mixture of ethyl acetate and hexane (1:4) to get a yellow solid (3.90 g, 85%).

^{1}H NMR (300 MHz, CDCl3): δ (ppm) 9.88 (s, 2H), 7.61 (s, 2H), 1.94 (m, 4H), 0.96–0.86 (m, 18H), 0.71 (m, 6H), 0.55 (t, $J = 7.2$ Hz, 6H). ^{13}C NMR (75 MHz, CDCl3): δ (ppm) 182.41, 148.32, 143.61, 138.59, 135.38, 52.47, 46.23, 33.63, 33.12, 29.25, 26.43, 23.02, 14.12, 11.93. MS (FAB): m/z [M^+] 459; calcd m/z [M^+] 458.23. Anal. Calcd for $C_{27}H_{38}O_2S_2$: C, 70.69; H, 8.35. Found: C, 70.91; H, 8.44.

3,3′-Di-n-hexylsilylene-2,2′-bithiophene-5,5′-dicarbaldehyde (5)

Compound **5** was synthesized in a similar synthetic procedure as described for **2** by taking 3,3′-di-*n*-hexylsilylene-2,2′-bithiophene (**4**) (3.63 g, 10 mmol) instead of compound **1** to get the desired product as a yellow solid (3.53 g, 83%).

^{1}H NMR (300 MHz, CDCl3): δ (ppm) 9.92 (s, 2H), 7.75 (s, 2H), 1.28–1.36 (m, 16H), 0.88–0.98 (m, 10H). ^{13}C NMR (75 MHz, CDCl3): δ (ppm) 183.12, 156.53, 147.30, 146.45, 139.07, 32.96, 31.53, 24.23, 22.69, 14.25,11.69. MS (FAB): m/z [M^+] 418; calcd m/z [M^+] 418.15. Anal. Calcd for $C_{22}H_{30}O_2S_2Si$: C, 63.11; H, 7.22. Found: C, 62.93; H, 7.07.

M1: To a mixture of compound **2** (1.15 g, 2.5 mmol) and 5-bromo-2-thiopheneacetonitrile (**3**) (2.02 g, 10 mmol) in methanol (100 mL), a catalytic amount of potassium tert-butoxide was added. The mixture was stirred at room temperature for 24 h. Then, the crude product was filtered and dried. Chromatography on silica gel eluted with CH_2Cl_2/hexane 1:4 afforded **M1** as a dark orange solid (1.71 g). Yield: 82%.

^{1}H NMR (300 MHz, CDCl3): δ (ppm) 7.57 (d, $J = 5.1$ Hz, 2H), 7.29 (d, $J = 11.1$ Hz, 2H), 7.09 (d, $J = 3.6$ Hz, 2H), 7.03 (d, $J = 3.9$ Hz, 2H), 1.96 (m, 4H), 0.97–0.90 (m, 18H), 0.79–0.73 (m, 6H), 0.72–0.61 (m, 6H). ^{13}C NMR (75 MHz, CDCl3): δ (ppm) 160.56, 142.20, 140.52, 133.27, 132.50, 127.18, 126.96, 123.14, 118.49, 105.59, 54.47, 43.32, 35.57, 34.35, 28.70, 27.56, 22.99, 14.28, 10.89. MS (FAB): m/z [M^+] 827; calcd m/z [M^+] 826.83. Anal. Calcd for $C_{39}H_{42}Br_2N_2S_4$: C, 56.65; H, 5.12; N, 3.39. Found: C, 56.91; H, 5.44; N, 3.65.

M2: M2 was synthesized in a similar synthetic procedure as described for **M1** by taking compound **5** (1.05 g, 2.5 mmol) to get a purple solid (1.45 g). Yield: 73%.

^{1}H NMR (300 MHz, CDCl3): δ (ppm) 7.57 (d, $J = 4.8$ Hz, 2H), 7.31 (d, $J = 9$ Hz, 2H), 7.1 (d, $J = 3.6$ Hz, 2H), 7.03 (d, $J = 3.9$ Hz, 2H), 1.10–1.62 (m, 16H), 0.92–0.73 (m, 10H). ^{13}C NMR (75 MHz, CDCl3): δ (ppm) 147.25, 142.01, 138.85, 133.12, 131.41, 129.28, 127.42, 116.48, 113.38, 103.07, 59.17, 33.21, 31.59, 23.18, 22.75, 18.57, 14.28. MS (FAB): *m/*

z [M^+] 786; calcd *m/z* [M^+] 786.80. Anal. Calcd for $C_{34}H_{34}Br_2N_2S_4Si$: C, 51.90; H, 4.36; N, 3.56. Found: C, 51.97; H, 4.85; N, 3.46.

4,4-Bis(2-ethylhexyl)-2,6-bis(trimethylstannanyl)-4H-cyclopenta-[2,1-b:3,4-b′]dithiophene (6)

This monomer was synthesized via the reported procedure,[5(b)] which was obtained as a light brownish viscous oil.

^{1}H NMR (300 MHz, CDCl3): δ (ppm) 6.93 (m, 2H), 1.86 (m, 4H), 1.29 (m, 2H), 0.94 (m, 16H), 0.78 (t, J = 6.8 Hz, 6H), 0.62 (t, J = 7.3 Hz, 6H), 0.37 (m, 18H). ^{13}C NMR (75 MHz, CDCl3): δ (ppm) 160.12, 143.04, 136.60, 130.52, 52.78, 43.57, 35.56, 34.91, 29.18, 28.07, 23.28, 14.63, 11.26, −7.79. MS (FAB) *m/z* [M^+] 728.0 calcd *m/z* [M^+] 728.2. Anal. Calcd for $C_{31}H_{54}S_2Sn_2$: C, 51.12; H, 7.47. Found: C, 51.47; H, 7.30.

5,5′-Bis(trimethylstannyl)-3,3′-di-n-hexylsilylene-2,2′-bithiophene (7)

This monomer was synthesized according to the literature procedure,[14(f)] which was obtained as a viscous oil.

^{1}H NMR (300 MHz, CDCl3): δ (ppm) 7.08 (s, 2H), 1.23–1.28 (m, 16H), 0.83–0.88 (m, 10H), 0.36 (s, 18H). ^{13}C NMR (75 MHz, CDCl3): δ (ppm) 155.22, 143.32, 137.89, 125.03, 33.11, 31.65, 24.47, 22.83, 14.33, 12.22, −7.87. MS (FAB) *m/z* [M^+] 418.0 calcd *m/z* [M^+] 418.15. Anal. Calcd for $C_{26}H_{46}S_2SiSn_2$ (%): C, 45.37; H, 6.74. Found (%): C, 46.69; H, 6.82.

General Polymerization Procedure

In a 25 mL flame-dried flask, 1.0 mmol of dibromo monomers **M1** or **M2** and 1.0 mmol of distannyl compounds **6** or **7** were added in 15 mL of anhydrous toluene and degassed with argon for 30 min. The Pd(0) complex, that is, tetrakis (triphenylphosphine)palladium (1 mol %), was transferred into the mixture in a dry environment. After another flushing with argon for 20 min, the reaction mixture was heated to reflux for 18 h. Then, an excess amount of 2-bromothiophene was added to end-cap the trimethylstannyl groups and reacted for 2 h. The reaction mixture was cooled to 40 °C and added slowly into a vigorously stirred mixture of methanol/acetone (3:1). The polymers were filtered through a Soxhlet thimble and then subjected to Soxhlet extraction with methanol, hexane, acetone, and chloroform. The polymers were recovered as solids from chloroform fraction by rotary evaporation and reprecipitation into methanol solutions. The solids were dried under vacuum for 1 day. The yields, ^{1}H NMR data, and molecular weights of the polymers are listed as follows:

CPDT-CN: Yield: 66%. ^{1}H NMR (300 MHz, CDCl3): δ (ppm) 7.65–7.29 (br, m, 6H), 7.20–6.89 (br, m, 4H), 2.01 (br, m, 8H), 1.02–0.67 (br, m, 60H). Anal. Calcd: C, 71.86; H, 7.54; N, 2.62. Anal. Found: C, 71.46; H, 7.35; N, 2.50. M_n = 16.4 K; Polydispersity Index (PDI) = 1.34.

DTS-CN: Yield: 59%. ^{1}H NMR (300 MHz, CDCl3): δ (ppm) 7.75–7.34 (br, m, 6H), 7.10–6.79 (br, m, 4H), 1.26 (br, m, 32H), 0.87 (br, m, 20H). Anal. Calcd: C, 65.54; H, 6.52; N, 2.83. Anal. Found: C, 64.68; H, 6.91; N, 2.39. M_n = 15.6 K; PDI = 1.86.

RESULTS AND DISCUSSION

Synthesis and Structural Characterization

The general synthetic procedures for monomers and polymers are outlined in Scheme 1. Compounds **1** or **4** were treated with Vilsmeier reagent to produce the corresponding dicarbaldehyde compounds. Then those compounds (**2** or **5**) were carried out condensation reaction with 5-bromo-2-thiopheneacetonitrile (**3**) in presence of catalytic amounts of potassium-tert-butoxide to form monomers **M1** and **M2**, respectively. All monomers (**M1, M2**, **6**, and **7**) were satisfactorily characterized by ^{1}H NMR, ^{13}C NMR, MS spectroscopy, and elemental analyses. Further Stille coupling reaction of corresponding distannyl compounds (**6** or **7**) with **M1** and **M2** in toluene using $Pd(PPh_3)_4$ as a catalyst at 110 °C for 18 h, polymers **CPDT-CN** and **DTS-CN** were acquired with yields of 66% and 59%, respectively. After purification in the Soxhlet extraction by leaving insoluble materials with high molecular weights, all polymers are soluble in organic solvents like $CHCl_3$, THF, chlorobenzene, and 1,2-dichlorobenzene at room temperature. The molecular weights of polymers were determined by GPC against polystyrene standards in THF eluent. Both the polymers have a similar number-average molecular weight (M_n) of 1.6 × 10^4 with PDI ranging 1.34–1.86. Because of the rigid thiophene and cyano groups of polymers, they have smaller molecular weights than the other polymers containing CPDT or DTS units. The thermal stabilities of the polymers were investigated by thermogravimetric analysis (TGA) under nitrogen (Fig. 1). Compared with **CPDT-CN** (414 °C), **DTS-CN** (430 °C) shows a higher decomposition temperature. Detailed GPC data and decomposition temperatures are summarized in Table 1. Nevertheless, both the polymers have good thermal stabilities, which are important in BHJ solar cell device fabrications and other applications.

Optical Properties

The photophysical characteristics of the polymers were investigated by ultraviolet–visible (UV–vis) absorption spectroscopy in dilute chloroform solutions (10^{-6} M) and solid films (spin-coated on quartz substrates). Figure 2 shows the absorption spectra of polymers, and the optical data including the maximum absorption wavelengths ($\lambda_{max,abs}$), absorption edge wavelengths ($\lambda_{edge,abs}$), and their optical band gaps (E_g^{opt}) in both solutions and films are summarized in Table 2. All absorption spectra appeared as broad absorption bands from 350 to 800 nm, which are more essential for the overlaps of the absorption spectra of the active layer with the solar emission. Reflecting much longer effective conjugation lengths of the extended coplanar CPDT- and DTS-based polymer backbones, the maximum absorption wavelengths ($\lambda_{max,abs}$) were 604 and 612 nm in solutions and at 621 and 628 nm in solid films for **CPDT-CN** and **DTS-CN**, respectively, which were more red shifted from the corresponding absorption wavelengths of monomers (459 and 473 nm for **M1** and **M2**, respectively). It is noted that both polymers exhibited maximum absorption wavelengths, longer than those of corresponding homopolymers (565 and 502 nm for polycyclopentadithiophene **PCPDT** and polydithienosilole

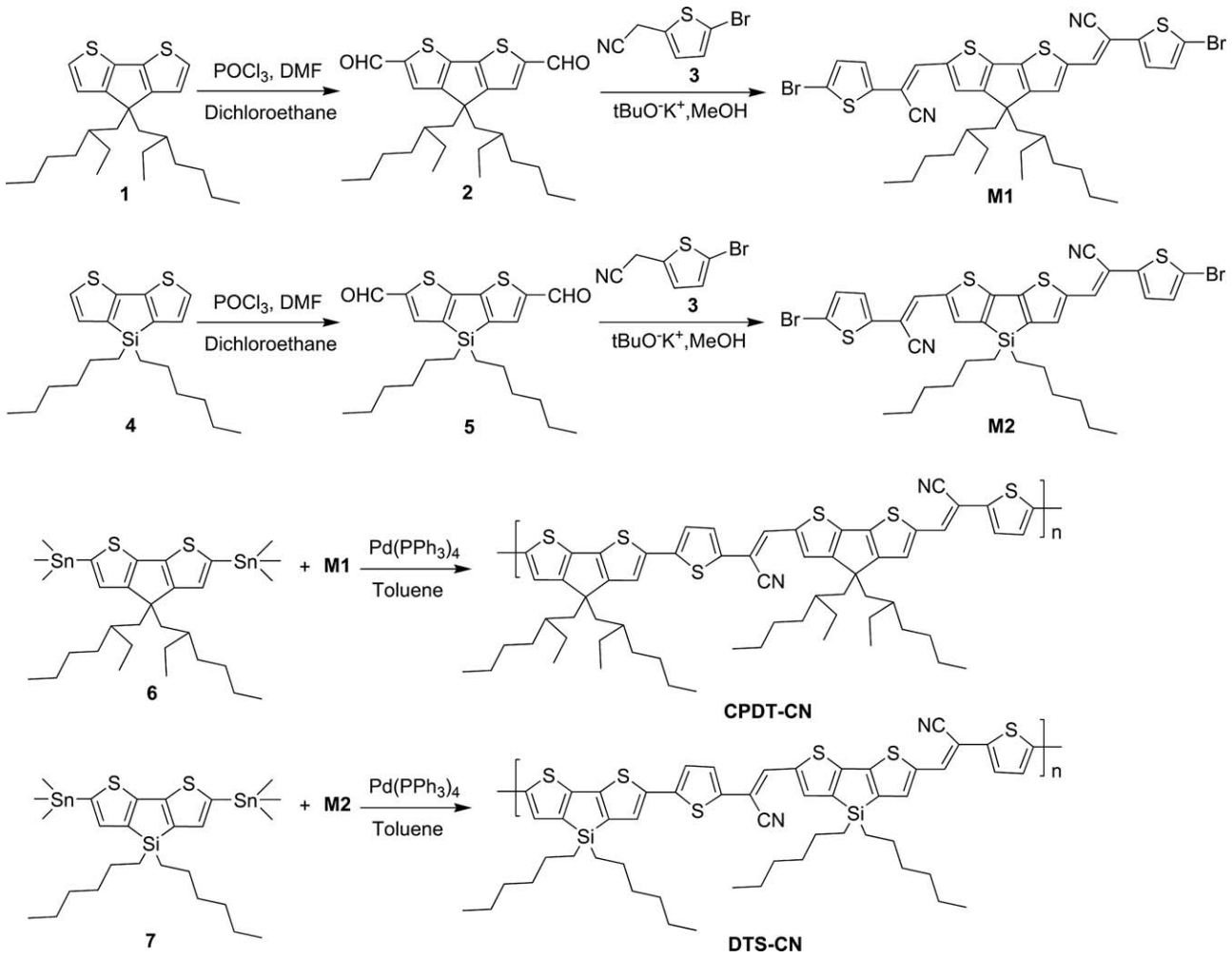

SCHEME 1 Synthetic routes for monomers and polymers.

PDTS, respectively),[20] which could be attributed to the strong ICT interactions between donor and acceptor moieties along with the formation of more rigid polymers in the presence of cyano-vinylene groups. Because of the inter-chain associations and π–π stackings of these polymers in solid state, the π–π^* transitions were red shifted (ca. 17 nm) in solid films than those in the corresponding solutions. The optical band gaps (E_g^{opt}) of the polymers determined by the absorption edges of UV–vis spectra in solid films were 1.65 and 1.56 eV for **CPDT-CN** and **DTS-CN**, respectively, which have the similar trends as the maximum absorption wavelengths. In brief, **DTS-CN** possessed the smallest band gap

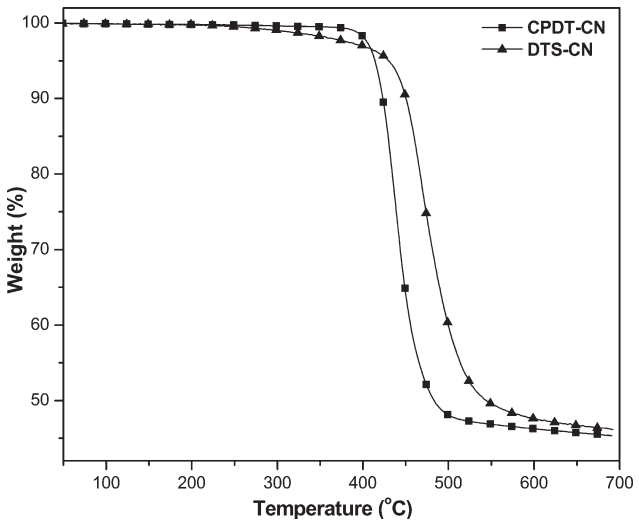

FIGURE 1 TGA measurements of polymers at a heating rate of 10 °C/min.

TABLE 1 Molecular Weights and Thermal Properties of Polymers

Polymer	Yield (%)	M_n[a] ($\times 10^3$)	M_w[a] ($\times 10^3$)	PDI[a] (M_w/M_n)	T_d[b] (°C)
CPDT-CN	66	16.4	22.0	1.34	414
DTS-CN	59	15.6	28.9	1.86	430

[a] Molecular weights (M_n and M_w) and PDI values were measured by GPC, using THF as an eluent, polystyrene as a standard.
[b] Temperature (°C) at 5% weight loss measured by TGA at a heating rate of 10 °C/min under nitrogen.
M_n, number average molecular weight; M_w, weight average molecular weight.

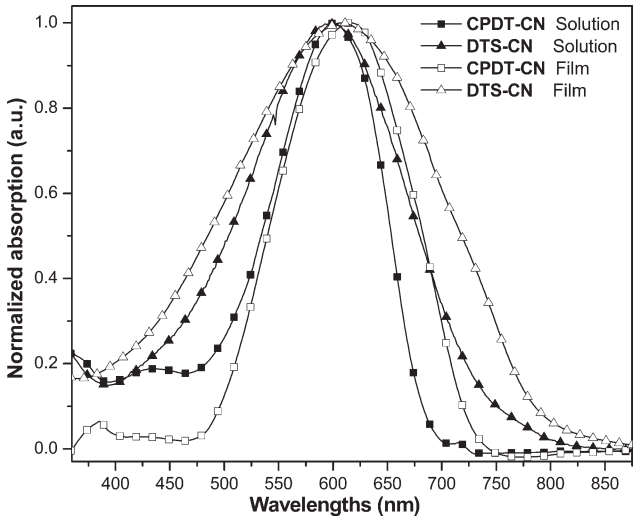

FIGURE 2 Normalized absorption spectra of polymers in dilute chloroform solutions (10^{-6} M) and solid films.

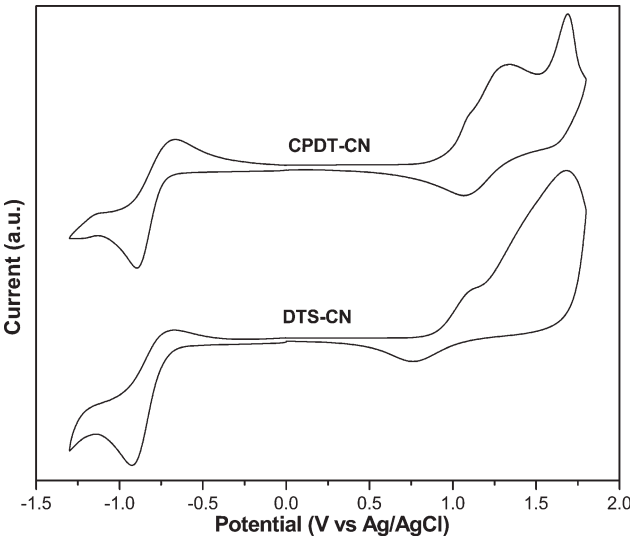

FIGURE 3 Cyclic voltammograms of polymers in solid films at a scan rate of 100 mV/s.

due to the electron-rich dithienosilole donor units in combination with the cyano-vinylene acceptor groups linked via thiophene units, which promoted an efficient intra-molecular charge transfer and led to an extensive delocalization within the polymer backbones.[21]

Electrochemical Properties

To understand the charge injection processes of the polymers in the BHJ solar cell devices, cyclic voltametry (CV) measurements are widely employed to investigate the redox behavior and to estimate the electronic states, that is, HOMO and LUMO energy levels of conjugated polymers.[22] In this regard, the cyclic voltograms of polymers are illustrated in Figure 3 and the related data are summarized in Table 2. Ag/AgCl was served as a reference electrode and it was calibrated by ferrocene [$E_{1/2(FC/FC^+)} = 0.45$ eV vs. Ag/AgCl]. The HOMO and LUMO energy levels were estimated by the oxidation and reduction potentials from the reference energy level of ferrocene (4.8 eV below the vaccum level) according to the following equation:[6]

$$E_{HOMO}/E_{LUMO} = [-(E_{onset} - E_{onset(FC/FC^+ \text{ vs. } Ag/Ag^+)}) - 4.8] \text{ eV}$$

where 4.8 eV is the energy level of ferrocene below the vacuum level and $E_{onset(FC/FC^+ \text{ vs. } Ag/Ag^+)} = 0.4$ eV. It can be seen from Figure 3 that both polymers exhibited similar two quasi-reversible or reversible *p*-doping/dedoping processes at positive potentials (ca. 1.1 V and 1.7 V) and one reversible *n*-doping/dedoping (reduction/reoxidation) process at negative potentials (ca. −0.8 V), which are good signs of high structural stability in the charged state. The onset oxidation potentials ($E_{ox/onset}$) of polymers **CPDT-CN** and **DTS-CN** were 0.88 V and 0.90 V, and the onset reduction potentials ($E_{red/onset}$) were −0.78 and −0.70 V, respectively. Polymers **CPDT-CN** and **DTS-CN** have the estimated HOMO levels of −5.28 and −5.30 eV and LUMO levels of −3.62 and −3.60 eV, correspondingly. As all HOMO levels were below the air oxidation threshold, the polymers should show good air stabilities.[23] It is also worthy noting that the electrochemical band gaps (E_g^{ec}, 1.66 and 1.60 eV for **CPDT-CN** and **DTS-CN**, respectively) calculated from $E_g^{ec} = (E_{ox/onset} - E_{red/onset})$ are in good agreements with the optical band gap values observed from UV–vis spectra (E_g^{opt}, 1.65 and 1.56 eV). All these electrochemical characteristics are within the desirable range for the ideal polymers to be utilized in the organic photovoltaic applications.

Photovoltaic Properties

To investigate the potential use of these polymers in polymer solar cell (PSC), the bulk heterojunction PSC devices with

TABLE 2 Optical and Electrochemical Properties of Polymers

	Absorption Spectra				Cyclic Voltammetry (vs Ag/Ag^+)				
	Solution[a]	Solid Film[b]			*p* Doping		*n* Doping		
Polymers	λ_{max} (nm)	λ_{max} (nm)	λ_{edge} (nm)	E_g^{opt} [c] (eV)	$E_{ox/onset}$ (V)	HOMO (eV)	$E_{red/onset}$ (V)	LUMO (eV)	E_g^{ec} (eV)
CPDT-CN	604	621	751	1.65	0.88	−5.28	−0.78	−3.62	1.66
DTS-CN	612	628	791	1.56	0.90	−5.30	−0.70	−3.60	1.60

[a] In dilute chloroform solution.
[b] Spin-coated from chlorobenzene solution.
[c] Optical band gap obtained from $E_g = 1240/\lambda_{edge}$.

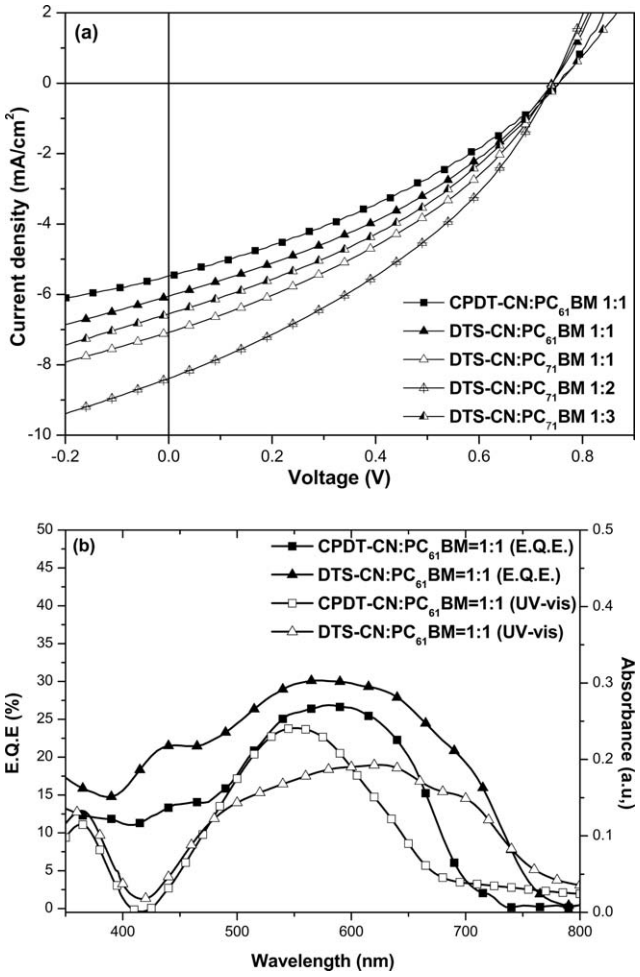

FIGURE 4 (a) Current–voltage curves of polymer solar cells using polymer:PCBM blends under the illumination of AM 1.5G, 100 mW/cm^2. (b) EQE and absorption spectra of the PSC devices based on polymers/PC$_{61}$BM (1:1, w/w).

a configuration of ITO/PEDOT:PSS/**CPDT-CN** or **DTS-CN**:PCBM/Ca/Al were fabricated from an active layer where, polymers were blended with PC$_{61}$BM in a weight ratio of 1:1 w/w initially. Later on, the active layer compositions were modified with various weight ratios for the optimum polymer **DTS-CN** with PC$_{71}$BM. Figure 4(a,b) illustrate the *J–V* curves (current density *J* vs. voltage *V*) and external quantum efficiency (EQE) curves as a function of wavelengths, respectively. The photovoltaic properties, that is, the values of open circuit voltage (V_{oc}), short circuit current density (J_{sc}), fill factor (FF), and PCE of BHJ solar cell devices are listed in Table 3. Because of negligible differences in HOMO levels of both polymers, they exhibited similar V_{oc} values (0.74–0.75 V) in the BHJ solar cell devices containing **CPDT-CN** or **DTS-CN**:PC$_{61}$BM in 1:1 weight ratio. With the similar V_{oc} values and FFs (33.9–35.7%), the PCE values of polymers **CPDT-CN** and **DTS-CN** were dependent on their J_{sc} values of 5.46 and 6.05 mA/cm^2, respectively. The PSC device based on the polymer blend of **DTS-CN**:PC$_{61}$BM (1:1 wt %) reached a higher PCE value of 1.60% with V_{oc} = 0.74 V, J_{sc} = 6.05 mA/cm^2, and FF = 35.7%. As reported, the more balanced hole and electron transporting properties as well as the higher hole mobilities are favorable factors for LBG polymers to be utilized in the solid films of BHJ solar cell devices,[24] so the PCE and J_{sc} values of the **DTS-CN**-based PSC device were higher than those based on **CPDT-CN**-based PSC device. This may be due to the higher hole mobility (9.82×10^{-4} cm^2/V/s) and more balanced charge transport (μ_e/μ_h = 1.6) in the polymer blend of **DTS-CN** compared with those (5.99×10^{-4} cm^2/V and 3.4, respectively) of the polymer blend of **CPDT-CN**. Furthermore, according to the absorption spectra of Figure 2 and EQE curves of Figure 4(b), it is evident that **DTS-CN** exhibited broader absorption bands and higher EQE values between 350 and 800 nm than those of **CPDT-CN**, which may be another reason for the higher J_{sc} value. As illustrated by the AFM images of polymer blends (1:1 weight ratio with PC$_{61}$BM) in Figure 5, due to the larger roughness of **DTS-CN** (1.48 nm) than that of **CPDT-CN** (0.67 nm), the higher PCE value of **DTS-CN**-based PSC device might be attributed to the film morphology accordingly.

Since the best performance of PSC device was observed in the previous optimum polymer blend of **DTS-CN**:PC$_{61}$BM (1:1 wt %) as an active layer, the PSC devices as a function of polymer blends **DTS-CN**:PC$_{71}$BM in various weight compositions were fabricated. Another electron acceptor PC$_{71}$BM was used to optimize the device properties due to its stronger light absorption in the visible region than that of PC$_{61}$BM.[25] The V_{oc} values observed in **DTS-CN**:PC$_{71}$BM solar cells were fairly stable in all polymer blend compositions (1:1–1:3 w/w) with PC$_{71}$BM, but the J_{sc}, FF, and PCE values are strongly dependent on the donor-to-acceptor weight

TABLE 3 Photovoltaic Properties of PSC Devices with the Configuration of ITO/PEDOT:PSS/Polymer:PCBM/Ca/Al

Active Layer	Hole Mobility (cm^2/Vs)	Electron Mobility (cm^2/Vs)	V_{oc} (V)	J_{sc} (mA/cm^2)	FF (%)	PCE (%)
CPDT-CN: PC$_{61}$BM = 1:1	5.99×10^{-4}	2.01×10^{-3}	0.75	5.46	33.9	1.39
DTS-CN: PC$_{61}$BM = 1:1	9.82×10^{-4}	1.65×10^{-3}	0.74	6.05	35.7	1.60
DTS-CN: PC$_{71}$BM = 1:1			0.74	7.07	35.9	1.89
DTS-CN: PC$_{71}$BM = 1:2			0.74	8.39	36.1	2.25
DTS-CN: PC$_{71}$BM = 1:3			0.75	6.55	36.5	1.79

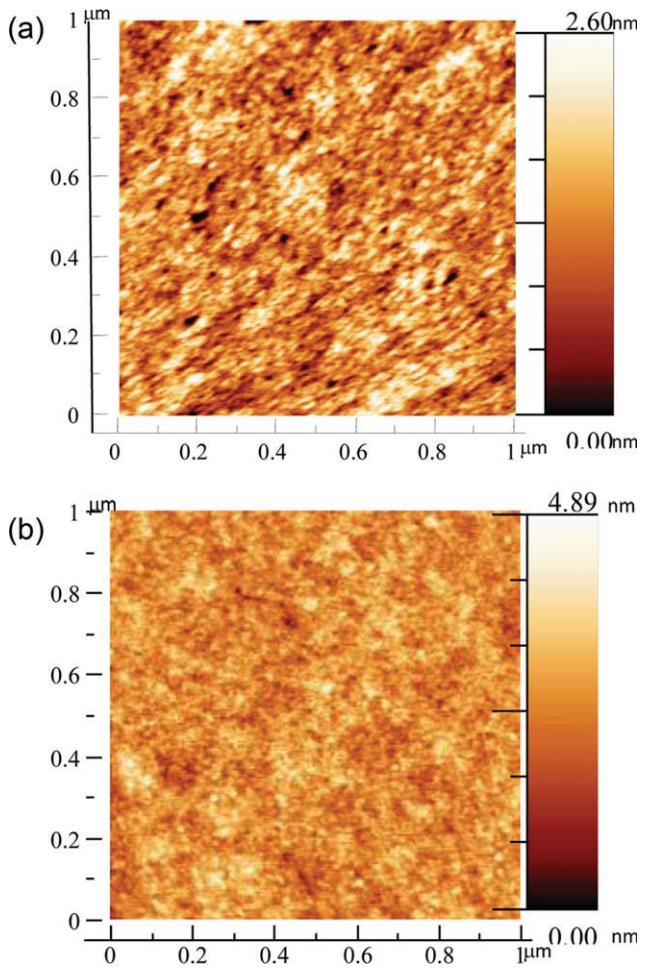

FIGURE 5 AFM images of (a) **CPDT-CN**: $PC_{61}BM$ 1:1 (w/w) and (b) **DTS-CN**: $PC_{61}BM$ 1:1 (w/w).

ratios in the active layers. The PSC device based on **DTS-CN**:$PC_{71}BM$ (1:2, w/w) exhibited the highest PCE = 2.25% with V_{oc} = 0.74 V, J_{sc} = 8.39 mA/cm^2, and FF = 36.1%. Though these polymers exhibited a higher J_{sc} compared with the other CPDT- and DTS-based polymers, their efficiencies were limited by their low FF and EQE values. Therefore, if the EQE values of the PSC devices can be enhanced by increasing the thickness of the active layer without hampering charge separation and transporting properties, the PSC device performance can be improved significantly. Low EQE values were also observed in some other LBG polymer systems, but this problem can be solved by developing new electron acceptor materials to replace PCBM.[26]

CONCLUSIONS

In summary, the concept of incorporation of electron deficient β-cyano-vinylene groups with donor–acceptor polymer architectures was utilized to improve the efficiencies of polymer solar cells. Cyano-vinylene groups were introduced via palladium(0)-catalyzed Stille coupling reactions into electron-rich building blocks, such as cyclopentadithiophene and dithienosilole to yield LBG polymers (**CPDT-CN** and **DTS-CN**). These polymers showed excellent charge-transporting properties with high hole mobilities in the range of 5.99–9.82 $\times$ 10^{-4} cm^2/V/s and good processabilities for PSC applications. Because of the lowest band gap and the highest hole mobility with more balanced charge transport of **DTS-CN** (with Si atom), an optimum PSC device based on the blended polymer **DTS-CN**:$PC_{71}BM$ = 1:2 (w/w) achieved the maximum PCE value up to 2.25%, with V_{oc} = 0.74 V, J_{sc} = 8.39 mA/cm^2, and FF = 36% (under AM 1.5 G 100 mW/cm^2). Regardless of the high open-circuit voltages and the large short-circuit currents of all PSC devices, the low FF values indicated the possibility of further device performance improvements by the optimization of film morphology of the polymer/PCBM blends and/or device architectures.

The authors are grateful to the National Center for High-Performance Computing for computer time and facilities. The financial supports of this project provided by the National Science Council of Taiwan (ROC) through NSC 97-2113-M-009-006-MY2, National Chiao Tung University through 97W807, and Energy and Environmental Laboratories (charged by Dr. Chang-Chung Yang) in Industrial Technology Research Institute (ITRI) are acknowledged.

REFERENCES AND NOTES

1 (a) Thompson, B. C.; Frechet, J. M. J. Angew Chem Int Ed Eng 2008, 47, 58–77; (b) Li, Y. F.; Zou, Y. P. Adv Mater 2008, 20, 2952–2958.

2 (a) Dennler, G.; Scharber, M.; Brabec, C. J. Adv Mater 2009, 21, 1323–1338; (b) Kim, J. Y.; Kim, S. H.; Lee, H.-H.; Lee, K.; Ma, W.; Gong, X.; Heeger, A. J. Adv Mater 2006, 18, 572–576; (c) Ma, W. L.; Yang, C.Y.; Gong, X.; Lee, K. H.; Heeger, A. J. Adv Funct Mater 2005, 15, 1617–1622.

3 (a) Hou, J. H.; Chen, H. Y.; Zhang, S. Q.; Chen, R. I.; Yang, Y.; Wu, Y.; Li, G. J Am Chem Soc 2009, 131, 15586–15587; (b) Chen, H.-Y.; Hou, J.; Zhang, S.; Liang, Y.; Yang, G.; Yang, Y.; Yu, Li.; Wu, Li.; Li, G. Nat Photonics 2009, 3, 649–653.

4 (a) Roncali, J. Chem Rev 1997, 97, 173–205; (b) Günes, S.; Neugebauer, H.; Sariciftci, N. S. Chem Rev 2007, 107, 1324–1338; (c) Cheng, Y. J.; Yang, S. H.; Hsu, C. S. Chem Rev 2009, 109, 5868–5923; (d) Bundgaard, E.; Krebs, F. C. Sol Energy Mater Sol Cells 2007, 91, 954–985; (e) Kroon, R.; Lenes, M.; Hummelen, J. C.; Blom, P. W. M.; de Boer, B. Polym Rev 2008, 48, 531–582.

5 (a) Blouin, N.; Michaud, A.; Gendron, D.; Wakim, S.; Blair, E.; Plesu, R. N.; Bellette, M.; Durocher, G.; Tao, Y.; Leclerc, M. J Am Chem Soc 2008, 130, 732–742; (b) Li, K. C.; Huang, J. H.; Hsu, Y. C.; Huang, P. J.; Chu, C. W.; Lin, J. T.; Ho, K. C.; Wei, K. H.; Lin, H. C. Macromolecules 2009, 42, 3681–3693; (c) Perzon, E.; Zhang, F.; Andersson, M.; Mammo, W.; Inganäs, O.; Andersson, M. R. Adv Mater 2007, 19, 3308–3311; (d) Huang, J. H.; Li, K. C.; Kekuda, D.; Padhy, H.; Lin, H. C.; Ho, K. C.; Chu, C. W. J Mater Chem 2010, 20, 3295–3300.

6 (a) Padhy, H.; Huang, J. H.; Sahu, D.; Patra, D.; Kekuda, D.; Chu, C. W.; Lin, H. C. J Polym Sci Part A: Polym Chem 2010, 48, 4823–4834; (b) Patra, D.; Sahu, D.; Padhy, H.; Kekuda, D.; Chu, C. W.; Lin, H. C. J Polym Sci Part A: Polym Chem 2010,

48, 5479–5489; (c) Sahu, D.; Padhy, H.; Patra, D.; Huang, J. H.; Chu, C. W.; Lin, H. C. J Polym Sci Part A: Polym Chem 2010, 48, 5812–5823.

7 Mühlbacher, D.; Scharber, M.; Morana, M.; Zhu, Z.; Waller, D.; Gaudiana, R.; Brabec, C. J. Adv Mater 2006, 18, 2884–2889.

8 Kim, Y.; Cook, S.; Tuladhar, S. M.; Choulis, S. A.; Nelson, J.; Durrant, J. R.; Bradley, D. D. C.; Giles, M.; McCulloch, I.; Ha, C.; Ree, M. Nat Mater 2006, 5, 197–203.

9 Lenes, M.; Wetzelaer, G. A. H.; Kooistra, F. B.; Veenstra, S. C.; Hummelen, J. C.; Blom, P. W. M. Adv Mater 2008, 20, 2116–2119.

10 Dennler, G.; Scharber, M.; Brabec, C. J. Adv Mater 2009, 21, 1323–1338.

11 Bredas, J. L.; Beljonne, D.; Coropceanu, V.; Cornil, J. Chem Rev 2004, 104, 4971–5003.

12 (a) Scharber, M. C.; Koppe, M.; Gao, J.; Cordella, F.; Loi, M. A.; Denk, P.; Morana, M.; Egelhaaf, H. J.; Forberich, K.; Dennler, G.; Gaudiana, R.; Waller, D.; Zhu, Z. G.; Shi, X. B.; Brabec, C. J. Adv Mater 2010, 22, 367–370; (b) Chen, H. Y.; Hou, J. H.; Hayden, A. E.; Yang, H.; Houk, K. N.; Yang, Y. Adv Mater 2010, 22, 371–375.

13 (a) Zhang, X.; Steckler, T. T.; Dasari, R. R.; Ohira, S.; Potscavage, W. J.; Tiwari, S. P.; Coppee, S.; Ellinger, S.; Barlow, S.; Bredas, J. L.; Kippelen, B.; Reynolds, J. R.; Marder, S. R. J Mater Chem 2010, 20, 123–134; (b) Zhang, S. M.; Fan, H. J.; Liu, Y.; Zhao, G. J.; Li, Q. K.; Li, Y. F.; Zhan, X. W. J Polym Sci Part A: Polym Chem 2009, 47, 2843–2852; (c) Zhan, X.; Tan, Z. A.; Zhou, E.; Li, Y.; Misra, R.; Grant, A.; Domercq, B., Zhang, X.-H.; An, Z.; Zhang, X.; Barlow, S.; Kippelen, B.; Marder, S. R. J Mater Chem 2009, 19, 5794–5803.

14 (a) Beaujuge, P. M.; Pisula, W.; Tsao, H. N.; Ellinger, S.; Muellen, K.; Reynolds, J. R. J Am Chem Soc 2009, 131, 7514–7515; (b) Hou, J.; Chen, H. Y.; Zhang, S.; Li, G.; Yang, Y. J Am Chem Soc 2008, 130, 16144–16145; (c) Hou, J.; Chen, T. L.; Zhang, S.; Chen, H.-Y.; Yang, Y. J Phys Chem C 2009, 113, 1601–1605; (d) Huo, L.; Hou, J.; Chen, H.-Y.; Zhang, S.; Jiang, Y.; Chen, T. L.; Yang, Y. Macromolecules 2009, 42, 6564–6571; (e) Usta, H.; Lu, G.; Facchetti, A.; Marks, T. J. J Am Chem Soc 2006, 128, 9034–9035; (f) Lu, G.; Usta, H.; Risko, C.; Wang, L.; Facchetti, A.; Ratner, M. A.; Marks, T. J. J Am Chem Soc 2008, 130, 7670–7685.

15 (a) Shi, W.; Fan, S. Q.; Huang, F.; Yang, W.; Liu, R. S.; Cao, Y. J Mater Chem 2006, 16, 2387–2394; (b) Hou, J. H.; Huo, L. J.; He, C.; Yang, C. H.; Li, Y. F. Macromolecules 2006, 39, 594–603; (c) Amir, E.; Sivanandan, K.; Cochran, J. E.; Cowart, J. J.; Ku, S. Y.; Seo, J. H.; Chabinyc, M. L.; Hawker, C. J. J Polym Sci Part A: Polym Chem 2011, 49, 1933–1941.

16 (a) Halls, J. J. M.; Walsh, C. A.; Greenham, N. C.; Marseglla, E. A.; Friend, R. H.; Moratti, S. C.; Holmes, A. B. Nature 1995, 376, 498–500; (b) Cardone, A.; Martinelli, C.; Pinto, V.; Babudri, F.; Losurdo, M.; Bruno, G.; Cosma, P.; Naso, F.; Farinola, G. M. J Polym Sci Part A: Polym Chem 2010, 48, 285–291.

17 (a) Greenham, N. C.; Moratti, S. C.; Bradley, D. D. C.; Friend, R. H.; Holmes, A. B. Nature 1993, 365, 628–630; (b) Kraft, A.; Grimsdale, A. C.; Holmes, A. B. Angew Chem Int Ed 1998, 37, 402–428; (c) Zhao, X.; Zhan, X. Chem Soc Rev ASAP, DOI: 10.1039/c0cs00194e; (d) Takagi, K.; Nakagawa, T.; Takao, H. J Polym Sci Part A: Polym Chem 2010, 48, 91–98.

18 Wan, M. X.; Wu, W. P.; Sang, G. Y.; Zou, Y. P.; Liu, Y. Q.; Li, Y. F. J Polym Sci Part A: Polym Chem 2009, 47, 4028–4036.

19 (a) Hou, J. H.; Tan, Z.; He, Y. J.; Yang, C. H.; Li, Y. F. Macromolecules 2006, 39, 4657–4662; (b) Sang, G.; Zhou, E.; Huang, Y.; Zou, Y.; Zhao, G.; Li, Y. J Phys Chem C 2009, 113, 5879–5885; (c) Zou, Y. P.; Liu, B.; Li, Y. F.; He, Y. H.; Zhou, K. C.; Pan, C. Y. J Mater Sci 2009, 44, 4174–4180; (d) Zou, Y. P.; Sang, G. Y.; Zhou, E. J.; Li, Y. F. Macromol Chem Phys 2008, 209, 431–438; (e) Shen, P.; Sang, G. Y.; Lu, J. J.; Zhao, B.; Wan, M. X.; Zou, Y. P.; Li, Y. F.; Tan, S. T. Macromolecules 2008, 41, 5716–5722; (f) Mikroyannidis, J. A.; Stylianakis, M. M.; Cheung, K. Y.; Fung, M. K.; Djurišić, A. B. Synth Met 2009, 159, 142–147; (g) Li, K. C.; Hsu, Y. C.; Lin, J. T.; Yang, C. C.; Wei, K. H.; Lin, H. C. J Polym Sci Part A: Polym Chem 2009, 47, 2073–2092.

20 (a) Liao, L.; Dai, L.; Smith, A.; Durstock, M.; Lu, J.; Ding, J.; Tao, Y. Macromolecules 2007, 40, 9406–9412; (b) Asawapirom, U.; Scherf, U. Macromol Rapid Commun 2001, 22, 746–749.

21 Kim, J. Y.; Qin, Y.; Stevens, D. A.; Ugurlu, O.; Kalihari, V.; Hillmyer, M. A.; Frisbie, C. D. J Phys Chem C 2009, 113, 10790–10797.

22 (a) Bard, A. J.; Faulkner, L. R. Electrochemical Methods: Fundamentals and Applications, 2nd ed.; Wiley: New York, 2001; (b) Thompson, B. C.; Kim, Y. G.; Reynolds, J. R. Macromolecules 2005, 38, 5359–5362.

23 de Leeuw, D. M.; Simenon, M. M. J.; Brown, A. R.; Einhard, R. E. F. Synth Met 1997, 87, 53–59.

24 Huang, J. H.; Ho, Z. Y.; Kekuda, D.; Chang, Y.; Chu, C. W.; Ho, K. C. Nanotechnology 2009, 20, 025202, 1–9.

25 (a) Wienk, M. M.; Kroon, J. M.; Verhees, W. J. H.; Knol, J.; Hummelen, J. C.; van Hal, P. A.; Janssen, R. A. J Angew Chem Int Ed 2003, 42, 3371–3375; (b) Yao, Y.; Shi, C.; Li, G.; Shrotriya, V.; Pei, Z.; Yang, Y. Appl Phys Lett 2006, 89, 153507, 1–3.

26 Wang, X. J.; Perzon, E.; Delgado, J. L.; de la Cruz, P.; Zhang, F. L.; Langa, F.; Andersson, M.; Ingans, O. Appl Phys Lett 2004, 85, 5081–5083.